EFFECT OF BEAM CURRENT, WELD SPEED AND DISSOLUTION ON MECHNICAL AND MICROSTRUCTURAL PROPERTIES IN ELECTRON BEAM WELDING

Akhilesh Krishnan[1], Anusha Rao Poduri[2], Seri Abhilash Reddy[3]

[1, 2, 3]*Undergraduate Student, Mechanical Engineering, Chaitanya Bharathi Institute of Technology, A.P, India,*
akhilesh.krishnan.cbit@gmail.com**, **anusha.poduri@gmail.com**, **abhilash.seri@gmail.com

Abstract

Electron beam welding has proved phenomenal in welding of components used in space because it uses a vacuum environment which eliminates substances like oxygen, nitrogen, and hydrogen. The main advantage of EBW is its ability to weld dissimilar materials and incorporate desirable properties in the assembly. It has high depth to width ratio and focuses exactly on the portion to be welded, thereby reducing the weld area, making it one of the most suitable welding processes. In this study, welding has been done on a circular heterogeneous component using an electron beam welding machine to determine the effect of beam current, speed of weld and dissolution on the bead geometry, hardness at the weld bead and the heat affected zone. This component is made up of AISI 304(Austenitic) and AISI 446 (Ferrite) stainless steel, both of which are widely used in space applications.

Index Terms: *Electron beam welding, AISI 304L, AISI 446, Beam current, Weld speed*

----------***----------

1. INTRODUCTION

1.1 Electron Beam Welding

Electron beam welding is defined as a fusion welding process where in coalescence is produced by the heat obtained from a concentrated beam composed primarily of high velocity electrons which strike the surfaces to be joined. Their kinetic energy changes to thermal energy thereby causing the work piece metal to fuse.

An electron beam consists of a tungsten filament, cathode (control) electrode, anode and focusing coil. A stream of electrons is generated by heating a tungsten filament, accelerated by a high voltage between the filament (cathode) and the anode. The beam may be accurately adjusted (by two pairs of x and y axis) by controlling the current flow through the deflection coils. The whole of the gun and work chamber are maintained in vacuum to prevent high voltage discharges between anode and cathode and also to prevent oxide contamination of the weld and surface of the work piece.

Gun discharges can cause serious weld defects if the electron gun is not kept continuously pumped to a higher vacuum than the chamber vacuum by diffusion pump via valve. The beam creates a key hole weld consisting of a molten zone with a hollow center containing hot solid metal but vapor supporting the molten part. If the beam is suddenly switched off quick solidification takes place in the hole and causes defective weld. Therefore it is necessary that on a circular weld there is a small overlap to ensure completes 360 degrees fusion.

The beam current is controlled by altering the potential difference between the cathode and a bias grid (thermionic valve). This grid enables a smooth control of the beam power from a few watts to several kilo watts for setting the slope and the power level to achieve the desired weld penetration.

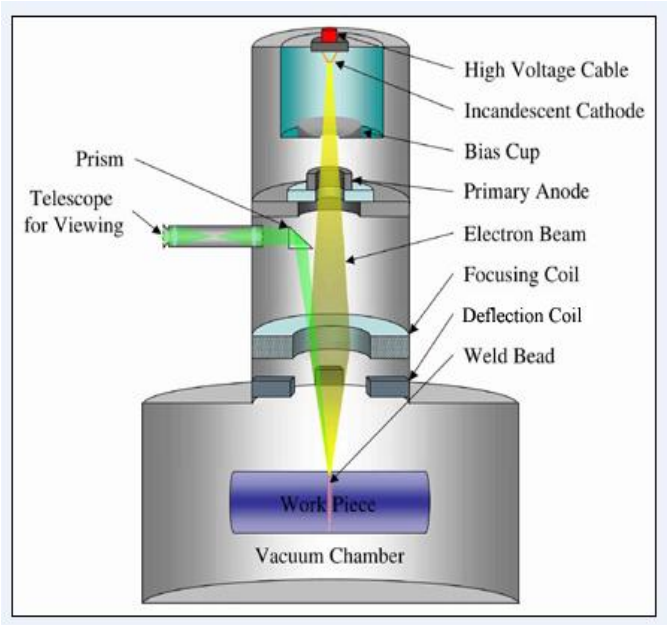

Fig-1: Electron Beam Welding Machine

2. EXPERIMENTAL SETUP

2.1 Electron Beam Welding Equipment

All the welding experiments were carried out in a 1cu meter electron beam welding machine of TECHMETA, France. This facility was provided in MTAR (Machine Tools Aids and Refurbishing) industries which is a leading production unit in space related components. The specifications of the machine are shown in the table 1.

Fig -2: Techmeta Electron Beam Welding Machine

Table-1: Specifications of EBW Machine

S.NO	Elements	Description
1	Vacuum chamber	Stainless steel (AISI-304L) 350 (H) x 360 (D)x 400 (L)
2	Chamber pumping system	Oil diffusion pump backed by rotary vane pump
3	E.B gun system	Indirectly heated cathode gun with 60 KV pump with dedicated vacuum system
4	Manipulation system	Gun vertical movement, rotary manipulator (radial weld), rotary manipulator (facial weld)
5	Gun vacuum	1x10-6 m bar
6	Year of commissioning	1978, subsequently augmented in 2005

2.2 Work Piece Preparation

The assembly used is that of a GSLV valve made of two different materials, namely AISI 304L and AISI 446, both of which are widely used in the space industry. The part with 304 series is austenitic in characteristic and that of 446 series is Ferrite in characteristic. The parts were manufactured on a CNC lathe and were press fitted. The thickness resulting from the mating of the two parts was found to be 1.85mm and the minimum depth required for welding is 1.35mm.

Once the work piece was made, they were cleaned with acetone, especially at the weld joint and were locked in the chuck of the EBW machine, the beam was focused on the spot to be welded taking the help of the viewing camera and the work piece was made ready for welding.

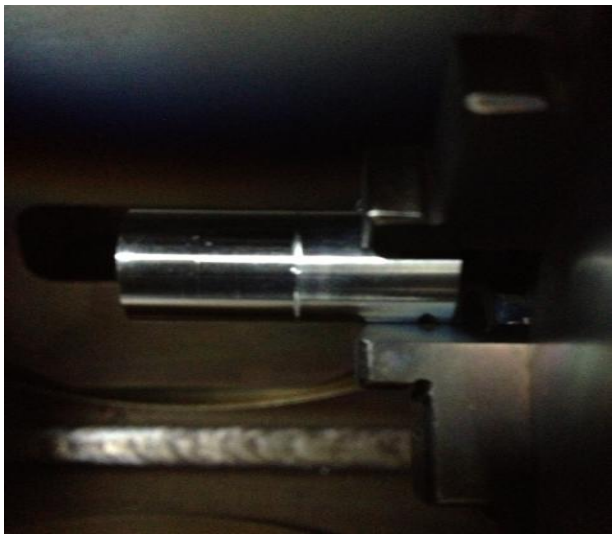

Fig- 3: Work piece loaded in the machine

3. TESTING TECHNIQUES

Various testing methods are used to determine the specifications (DOP), defects (blow holes, porosity) and mechanical properties (hardness) of the weld bead.

3.1 X ray Film Radiography

In this method, the part is placed between the radiation source and a piece of film. The part will stop some of the radiation. Thicker and denser area will stop more of the radiation. The film darkness (density) will vary with the amount of radiation reaching the film through the test object. The equipment is shown in figure 4.

Fig-4: Film Radiography Equipment

3.2 Dye Penetration Test

The dye penetration test is also a type of non destructive testing. It is a widely applied and low-cost inspection method used to locate surface-breaking defects in all non-porous materials (metals, plastics, or ceramics). The Penetrant may be applied to all non-ferrous materials and ferrous materials. DPI is used to detect welding surface defects such as hairline cracks, surface porosity, and fatigue cracks on in-service components. Penetrant may be applied to the test component by dipping, spraying, or brushing. After adequate penetration time has been allowed, the excess Penetrant is removed, a developer is applied. The developer helps to draw Penetrant out of the flaw where an invisible indication becomes visible to the inspector. Inspection is performed under ultraviolet or white light, depending upon the type of dye used in order to detect the defects, if any. The figure 5 show the DPI conducted on the specimens.

Fig-5: Dye Penetrant Test

3.3 Vickers Hardness Test or Micro Hardness Test

The Vickers hardness test method, also referred to as a micro hardness test method, is mostly used for small parts, thin sections, or case depth work. The Vickers method is based on an optical measurement system. The Micro hardness test procedure specifies a range of light loads using a diamond indenter to make an indentation which is measured and converted to a hardness value. A square base pyramid shaped diamond is used for testing in the Vickers scale. Typically loads are very light, ranging from a few grams to one or several kilograms. In the beam current and speed testing, the force applied is 300 grams force.

The diagonal length is calculated and hence the area of indent can be determined using the formula A=d2/1.8544 and the hardness is determined using the formula,

Hardness= Force/Area = 1.8544 F/d2.

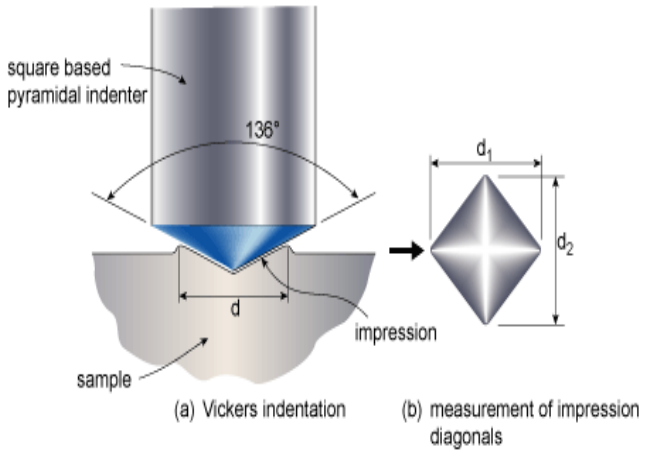

Fig-6: Vickers Hardness Test

3.4 Micro Structure Analysis

Microstructure and Analysis focuses on the art and science of preparing, interpreting, and analyzing microstructures in engineered materials, to better understand materials behavior and performance. In this experiment, specimens of thickness 1.5mm (by wire EDM) were prepared and were treated with Aquaregia and Pickers reagent to etch the weld bead. The main focus was to compare the presence of delta ferrite in the micro structures. The presence of delta ferrite above 12% increases the brittleness in the material and below 5% induces ductility in the material both of which are not suitable.

α ferrite is formed due to transformation of austenite at temperatures below 13900C but due to the high temperature of electron beam at approximately 23350C for a beam current 11.0mA and 2.3mA weld focus value and faster cooling rate of stainless steel, the α ferrite changes to a more stable body centered structured form of δ ferrite which is therefore

retained in the microstructure. The amount and distribution of δ ferrite is strongly affected by chemical composition of steel, but less affected by the cooling rate.

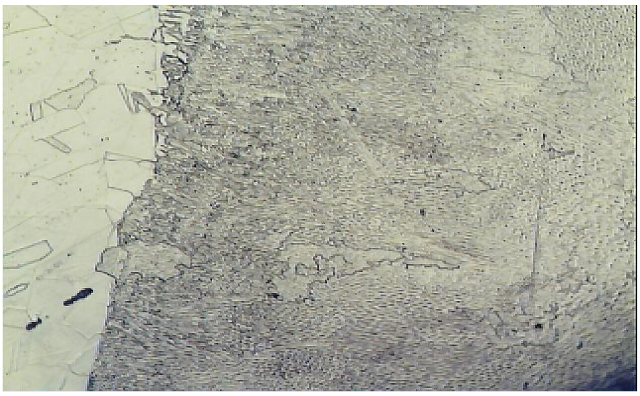

Fig-7: Microstructure at 200X

3.5 Depth of Penetration Using Optical Projector

The depths of penetration for the specimens were determined using a Mitutoyo optical projector as shown in figure 8.

Fig-8: Optical Projector

4. EXPERIMENTAL ANALYSIS

4.1 Beam Current Test

Beam current is one of the most vital parameters in the electron beam welding process. Experiment has been conducted to note its effects on the depth of penetration, hardness and the fusion of the two different materials in the micro structure. Trials were conducted, to determine the range of beam current that can be used for a thickness of 1.85mm. These trials were conducted without backing on the free end one of the component. The range is selected on the criterion that when there is a small impression or deep impression without backing, it will give a good weld with backing. Hence the range of beam currents is determined to be in between 10.5mA and 12mA. At constant voltage, weld focus value, speed of 1000 rpm, duration and vacuum, beam current was varied as tabulated in table 2 and observations were made.

Table-2: Beam Current Test

Experiment No	Voltage, U KV	Weld Focus Value, J Amps	Beam Current, I mA	Duration in degrees	Vacuum, mm of Hg
1	50	2.28	10.6	10/150/10/10	10-4
2	50	2.28	10.8	10/150/10/10	10-4
3	50	2.28	11.0	10/150/10/10	10-4
4	50	2.28	11.2	10/150/10/10	10-4
5	50	2.28	11.4	10/150/10/10	10-4
6	50	2.28	11.8	10/150/10/10	10-4

4.2 Results and Discussions of Beam Current Test

In order to determine the effects of the above experiments, various tests were conducted and their observations detailed and discussed.

4.2.1 Depth of Penetration

Using an optical projector, the depth of penetration was determined for each of the specimen and the variation is presented.

Table-3: Variation in DOP with Change in Beam Current

S.NO	Beam Current, mA	Depth of Penetration, mm
1	10.6	1.67
2	10.8	1.71
3	11.0	1.76
4	11.2	1.82
5	11.4	1.87
6	11.8	1.935

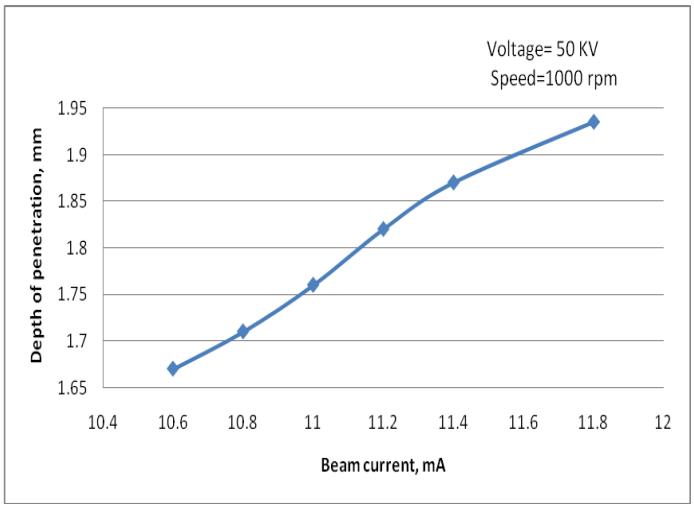

Fig-9: Variation in DOP with Beam Current

4.2.2 Visual Inspection

On visual inspection it was observed that spattering occurred in specimens with beam currents of 11.4mA and 11.8mA and also a small impression was observed in the specimen with beam current 11.2mA.

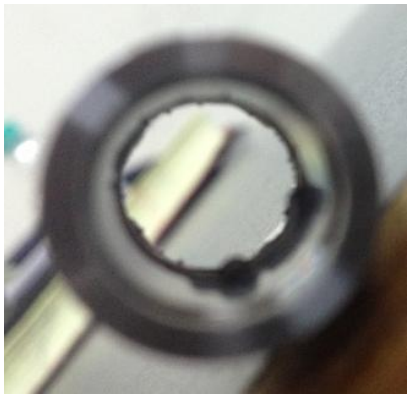

Fig-10: Spattering in Specimen with Beam Current 11.8ma

4.2.3 Dye Penetration Test

It was observed that there are no cracks or surface defects in any of the specimens.

4.2.4 X-ray Test

It was observed that the specimen with beam current 11.8mA has porosity in the weld pool and no internal defects like blowholes or porosity was found in the other specimens.

After the above three tests the specimens with beam currents 10.6, 11.2, 11.4, 11.8mA were not considered for further testing because of defects discussed above.

4.2.5 Micro Structure Analysis

Micro structure analysis was conducted on specimens with beam currents 10.8mA and 11.0mA. This is shown in figures 11 and 12.

1. Beam current: 10.8mA, speed: 1000 rpm
Observation: The depth of penetration is good. The microstructure consists of delta ferrite in the weld pool, within limits of 5-12% which is acceptable.

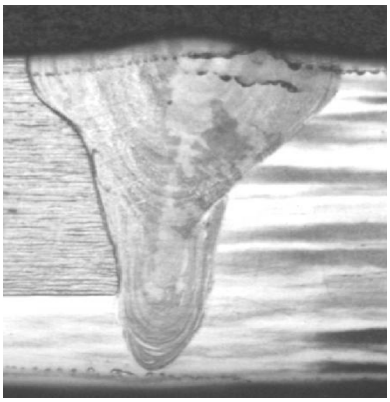

Fig-11: Microstructure of Weld with Beam Current 10.8mA at 200X

2. Beam Current: 11.0mA
Observation: There is not much difference in the depth of penetration and the amount of delta ferrite present in the microstructure when compared to the specimen with beam current 10.8mA.

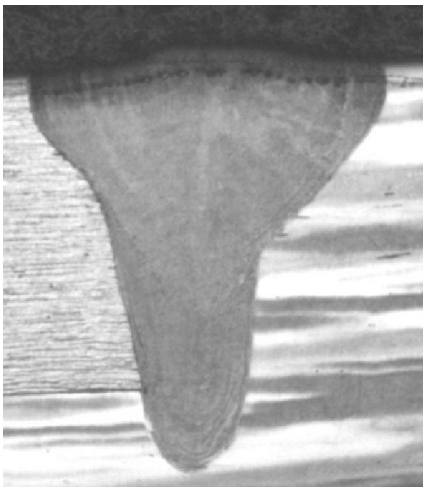

Fig-12: Microstructure of Weld with Beam Current 11.0mA at 200X

Hence in terms of micro structure analysis both specimens with beam currents 10.8mA and 11mA are satisfactory.

4.2.6 Hardness Test

Micro hardness test was conducted on the specimens with currents 10.8mA and 11.0mA. Hardness values at weld (average of the top, middle and bottom sections) and at the heat affected zone (average of values in the ferrite and austenite sections) was calculated and shown in table 5.4. The hardness of the parent material AISI 304L was found to be 192 HV and that of AISI 446 is 210 HV.

Table-4: Variation of Hardness with Beam Current

Specimen No.	Beam Current, mA	Hardness at sections, HV	Average Hardness, HV	Hardness at HAZ sections, HV		Average Hardness at HAZ, HV
				Ferrite	Austenite	
1	10.8	180,187,187	185	180	190	185
2	11.0	212,208,205	209	188	190	189

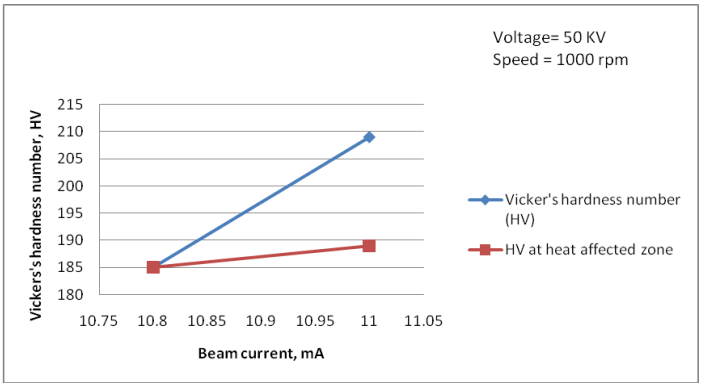

Fig-13: Variation in Hardness at Weld and HAZ with Increase in Beam Current

4.3 Speed Test

Welding speed: It is the speed with which the work piece is moved. As the welding speed increases, the weld will become narrow and the penetration will start to decrease. Further higher the speed, more quickly the molten metal will freeze behind the weld.

The aim of the experiment is to determine an optimum speed for welding the component. For this purpose the weld speed has been varied from 800 to 1400 rpm in steps of 200 rpm in order to determine its effect on the weld bead geometry and hardness. In this process all the other parameters like voltage, duration, weld focus value and the vacuum in the chamber has been kept constant. The beam current is kept constant at a value of 11.0mA which is an optimum value for the component of thickness 1.85mm as determined in section 4.1 (Beam current test).

Table-5: Speed Test

Experiment No	Voltage, U KV	Weld Focus Value, J Amps	Speed, F rpm	Duration in degrees	Remarks
1	50	2.28	800	10/150/10/10	Slight undercut
2	50	2.28	900	10/150/10/10	Bead is satisfactory
3	50	2.28	1000	10/150/10/10	Bead is satisfactory
4	50	2.28	1200	10/150/10/10	Bead is satisfactory
5	50	2.28	1400	10/150/10/10	Bead is satisfactory

4.4 Results and Discussions of Speed Test

In order to determine the effects of the above experiments, various tests were conducted and their observations were detailed and discussed.

4.4.1 Depth of Penetration

The depth of penetrations was obtained using an optical projector. The observations are tabulated and a graph is plotted to show the variations

Table-6: Variation in DOP with Change in Weld Speed

Specimen No.	Speed of weld, F rpm	Depth of penetration, mm
1	800	1.41
2	900	1.48
3	1000	1.76
4	1200	1.34
5	1400	1.32

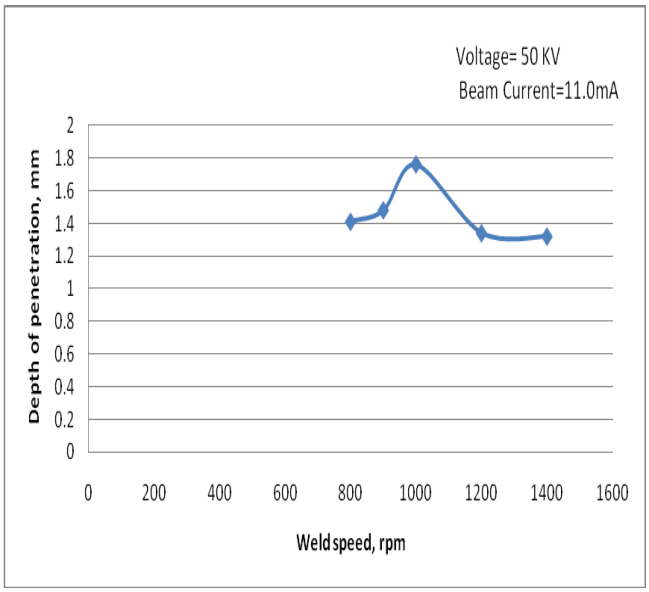

Fig-14: Variation in DOP with Increase in Weld Speed

4.4.2 Visual Inspection

On visual inspection it was observed that there was an undercut in the specimen with speed of weld 800 rpm because of the concentration of high energy electrons for a long time at a particular place.

4.4.3 Dye Penetration Test

It was observed that there are no cracks or surface defects in any of the specimens.

4.4.4 X-ray Test

It was observed that there are no internal defects like blowholes or porosity in any of the specimens.

4.4.5 Micro Structure Analysis

Micro structure analysis was conducted on specimens with weld speeds 900, 1000, 1200 and 1400 rpm to analyze the relative presence of delta ferrites in the micro structure.

1. Weld Speed: 900 rpm, Beam Current: 11.0mA
Observation: At this speed it is seen that there is a partial depth of penetration in the weld bead. There is an increase in the bead thickness as when compared to the bead with speed of 1000 rpm. There is a high amount of delta ferrite in the structure (>12%). This makes the material brittle. This can be attributed to having longer time duration of the beam at a spot.

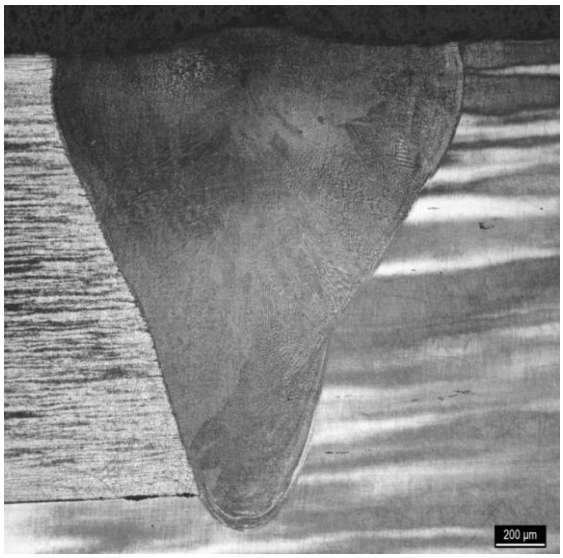

Fig-15: Micro structure of weld with weld speed 900 rpm

2. Weld speed: 1000 rpm, Beam current: 11.0mA
Observation: The weld has a minimal required spot size and has a suitable depth of penetration. The amount of delta ferrite has reduced when compared to the bead with speed of 900 rpm and is within the control range of 5-12%.

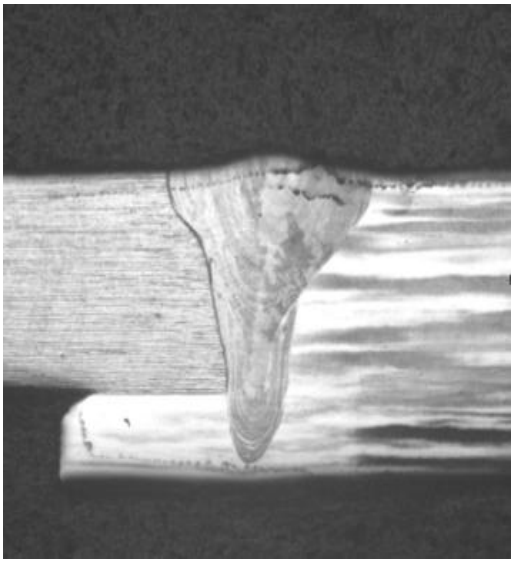

Fig-16: Micro structure of weld with weld speed 1000 rpm

3. Weld speed: 1200 rpm
Observation: The bead has not reached the minimum depth of penetration required and though there is increase in the width of the bead, the amount of delta ferrite is considerable less (lies in limits of 5-12%) and there is no significant reduction of hardness in the HAZ.

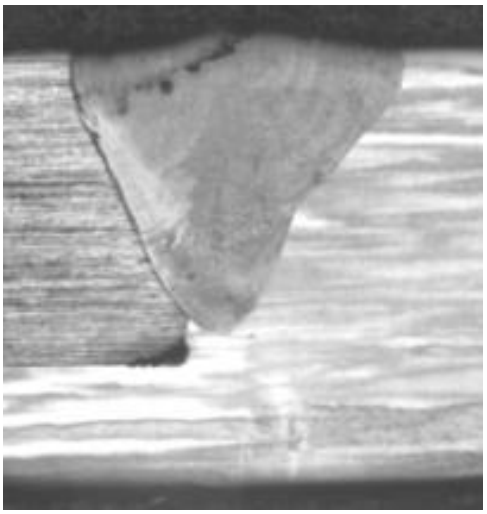

Fig-17: Micro structure of weld with weld speed 1200 rpm

4. Weld speed: 1400 rpm

Observation: It can be observed that there is a considerable increase in the width of the weld beam as when compared to the change in the depth of penetration and the HAZ is less and can be attributed to the low duration of the beam at a spot.

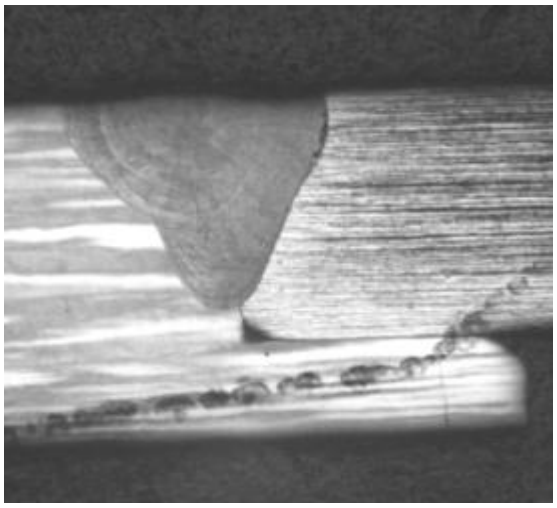

Fig-18: Micro structure of weld with weld speed 1400 rpm.

From the micro structure observations and depth of penetration tests, it is seen that at lower speeds of 800 and 900 rpm the increase in width of bead is high but the DOP is less even though the beam is focused at the spot for longer time. The reason for this may be the heating effect of the electron beam. This can be interpreted as being produced by a distributed, point or line heat source depending on the energy and power density of the electron beam. For an energy density below a critical value the weld behaves in a distributed source mode.

This critical energy, from literature was found to be a material dependent property. It is also noted that above the critical value, the weld behaves in a point source mode. Hence this can reason the skewed manner of DOP.

4.4.6 Hardness Test

Micro hardness test was conducted on the specimens with weld speeds of 900, 1000, 1200, and 1400 rpm. Hardness values at weld (average of the top, middle and bottom sections) and at the heat affected zone (average of values in the ferrite and austenite sections) was calculated and shown in table 5.7. The hardness of the parent material AISI 304L was found to be 192 HV and that of AISI 446 is 210 HV.

Table-7: Variation of Hardness in the weld and HAZ with change in weld speed

Specimen No.	Speed of weld, F rpm	Hardness at sections,	Average Hardness, HV	Hardness at HAZ sections,		Average Hardness at HAZ, HV
				Ferrite	Austenite	
1	900	195,200,190	195	180	190	185
2	1000	212,208,205	209	188	190	189
3	1200	192,190,191	191	186	202	194
4	1400	191,198,188	192.4	187	208	194.5

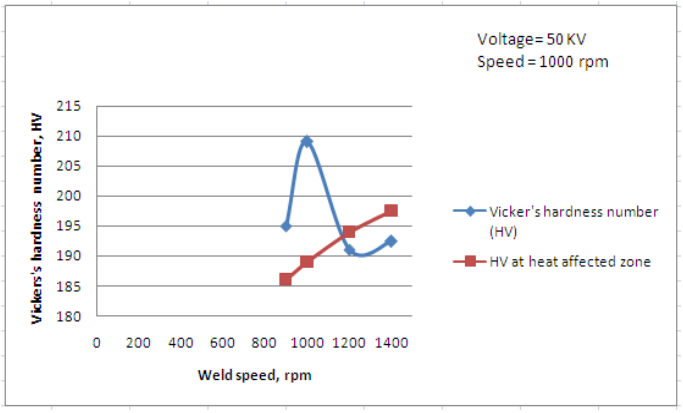

Fig-19: Variation in hardness at weld and HAZ with weld speed

4.5 Dissolution Test

Dissolution is the process of giving offset to the electron beam to either side of the weld (from the center) so as to impart the useful properties of the superior parent material into the weld. In this experiment an offset of 0.2mm has been given to the electron beam, either side of the center weld to observe the effect it has on the weld bead's hardness and microstructure. The beam current was reduced to 10.6mA after a number of trials because the other beam currents resulted in spattering due to the lack of backing at a distance of 0.2mm on either side of the weld, the weld speed was kept constant at 1000rpm during this experiment.

4.6 Results and Discussions in Dissolution Test

In order to determine the effects of the above experiments, various tests were conducted and their observations were detailed and discussed.

4.6.1 Depth of Penetration

The depth of penetrations for the shift of the beam towards the austenite and ferrite parts is shown in table 8.

Table-8: Depth of Penetration

Experiment No.	Shift Towards	Depth Of Penetration, mm
1	Austenite	1.76
2	Ferrite	1.76

4.6.2 Visual Inspection

When the components where visually inspected, there was no spattering that could be seen on either of the specimens indicating that the weld was good with no visual surface defects.

4.6.3 Dye Penetration Test

The die penetration test was conducted on the specimens and there were no surface defects that were detected. This indicates that there is perfect surface weld with no defects such as cracks.

4.6.4 X-ray Test

X-ray Test was conducted on the specimens and there were no internal defects (such as undercut, porosity) that were detected.

4.6.5 Microstructure Analysis

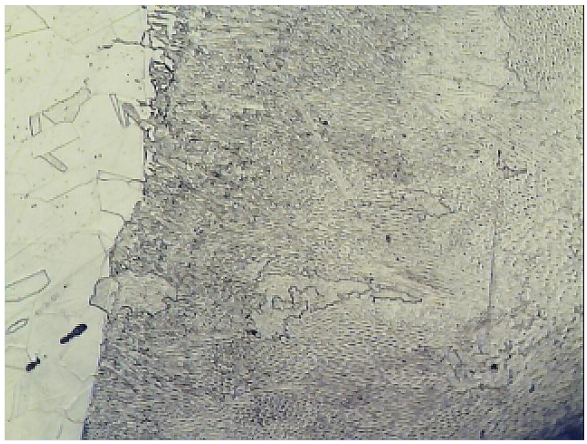

Fig-20: Micro structure-Austenite shift

The microstructure of the 1st specimen (shift towards austenite) consists of austenite dendrites and interdentric delta ferrite in the matrix of the austenite. The percentage of delta ferrite is in between 5-12%.

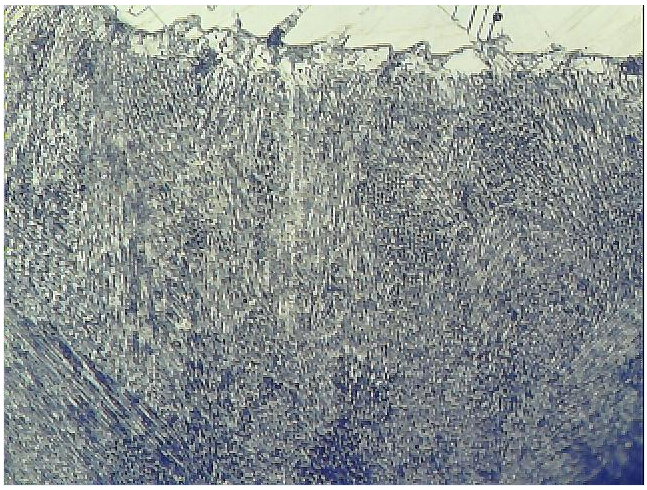

Fig-21: Micro Structure-Ferrite shift

The microstructure of the 2nd specimen (shift towards ferrite) consists of austenite dendrites and heavy interdentric delta ferrite in the matrix of the austenite. The percentage of delta ferrite is found to be greater than 12% and may cause brittleness in the material.

4.6.6 Hardness Test

Vickers Hardness test was conducted with a load of 5kg and a diamond indenter was used in this process. The hardness test was conducted at three sections of the weld area which are the top, center and the bottom of the weld pool. The average of the three values was taken and is shown in table 9.

Table-9: Hardness Results for Dissolution

Experiment No	Shift Towards	Hardness,1 HV	Hardness,2 HV	Hardness,3 HV	Average Hardness,HV
1	Austenite	148	152	150	150
2	Ferrite	177	172	175	174.67

It can be seen that the hardness can be improved by shifting the beam towards the ferrite region but compromising with the ductility of the material.

CONCLUSIONS

1. The depth of penetration increases with beam current and it is observed that for every 0.2mA increase in current, depth of penetration approximately increases by 0.05 mm.
2. The hardness (209 HV) is found to be highest at a beam current of 11.0mA and the hardness at heat affected zone in the austenitic half is observed to be 188 HV. This value of hardness is comparatively more when compared to that at a beam current of 10.8mA which is 180HV. Hence, the optimum beam current for the welding of this component can be concluded to be 11.0mA.
3. As the speed increases, the depth of penetration also increases, reaches a maximum value and then starts to decrease. This decrease in the DOP can be attributed to the reduced time duration at a spot due to high speeds.
4. At lower speeds, the increase in the width of the bead is more comparable than the increase in depth of penetration which is skewed from the expected. Due to the reduced time duration of the beam at higher speeds, the effect of HAZ on the hardness is less.
5. The presence of delta ferrite in the micro structure decreases with the increase in speed but there is a reduction in the DOP.
6. The dissolution test proves that shifting the beam towards the ferrite part gives a better hardness in the weld but at the same time increases the content of delta ferrite which makes the material ductile.

ACKNOWLEDGEMENTS

Firstly we would like to express our immense gratitude and heart full thanks towards our institution Chaitanya Bharathi Institute of Technology, which created a great platform to attain profound technical skills in the field of Mechanical Engineering, thereby fulfilling our most cherished goal.

We extend our heart full thanks to our project guide, Dr. P. Ravinder Reddy, Head of Mechanical Engineering Department for his excellent supervision, support and guidance. Without his supervision and many hours of devoted guidance, stimulating & constructive criticism, this thesis would never come out in this form.

We sincerely thank Mr.G Madhusudan Reddy for his valuable time and giving us permission to the facilities at DMRL.We also wish to thank MTAR industries for providing us with their valuable time, material and allowing us to complete our project on electron beam welding.

REFERENCES:

[1] James M Fragomeni, Arthur C.Nunes Jr., Study of the effects of welding parameters on EBW in space environment. Aerospace science and technology, Science direct,2003 373-384
[2] Ll Chun Xu HE Cheng dan,XU Qrjin,JIANG Car yun,Desing o0f electrostatic Focusing for space Electron Beam Welding Gun, Chinese journal of aeronautics vol 18,3
[3] Vidyut Dey,Dilip Kumar,GL Dutta,MN Jha,TK saha,AV bapat, Optimization of beam geometry in EBW using a genetic algorithm, ELSEVIER journal of materials processing technology 209(2009)1151-1157..
[4] Handbook of electron beam welding (Wiley series on the science and technology)
[5] Angelo Fernando Padilha, Caio Fazzioli Tauares, Marcelo Aquino Mautorano, Delta ferrite formation in austenite stainless steel casting, Material science forum vol 730-732 (2103)
[6] H.C Vacher and C.J Bechtoldt, Delta ferrite-austenite reactions and formation of carbide, sigma and chi phases in 18Cr-8Ni-3.5Mo steels, Journal of research of national bureau of standards, vol 53 no.2 aug 1954.
[7] J.W Elmer W.H Gedt and T.M Eagar, The transition from shallow to deep penetration during electron beam welding, Welding research, may 1990

BIOGRAPHIES:

Akhilesh Krishnan, He's an undergraduate student at Chaitanya Bharathi Institute of Technology, Hyderabad. Akhilesh is inclined towards the research in the field of Manufacturing, Non Conventional machining and Renewable energy development.

Anusha Rao Poduri, She is an undergraduate student at Chaitanya Bharathi Institute of Technology, Hyderabad. Areas of Interest: Manufacturing and Operations Research

Seri Abhilash Reddy He's an undergraduate student at Chaitanya Bharathi Institute of Technology, Hyderabad. Areas of Interest: Manufacturing and Renewable energy development.